CERPO

Centro de Referencia Perinatal Oriente

Facultad de Medicina, Universidad de Chile

Seminario N°87: Resonancia magnética fetal

Dr Heinz Dauelsberg Noemi, Dr. Daniel Martin Navarrete, Dra Paz Ahumada Droguett, Dr. Sergio de la Fuente Gallegos

Mayo 2022

INTRODUCCIÓN

- Herramienta diagnóstica complementaria fundamental al US.
- Permite evaluación de desarrollo cerebral fetal.
- No utilizada como herramienta primaria de tamizaje prenatal.
- Indicada luego de US experta con información fetal incompleta.

ISUOG Practice Guidelines: Performance of fetal magnetic resonance imaging. 2017

CERPO

isuog.org

GUIDELINES

ISUOG Practice Guidelines: performance of fetal magnetic resonance imaging

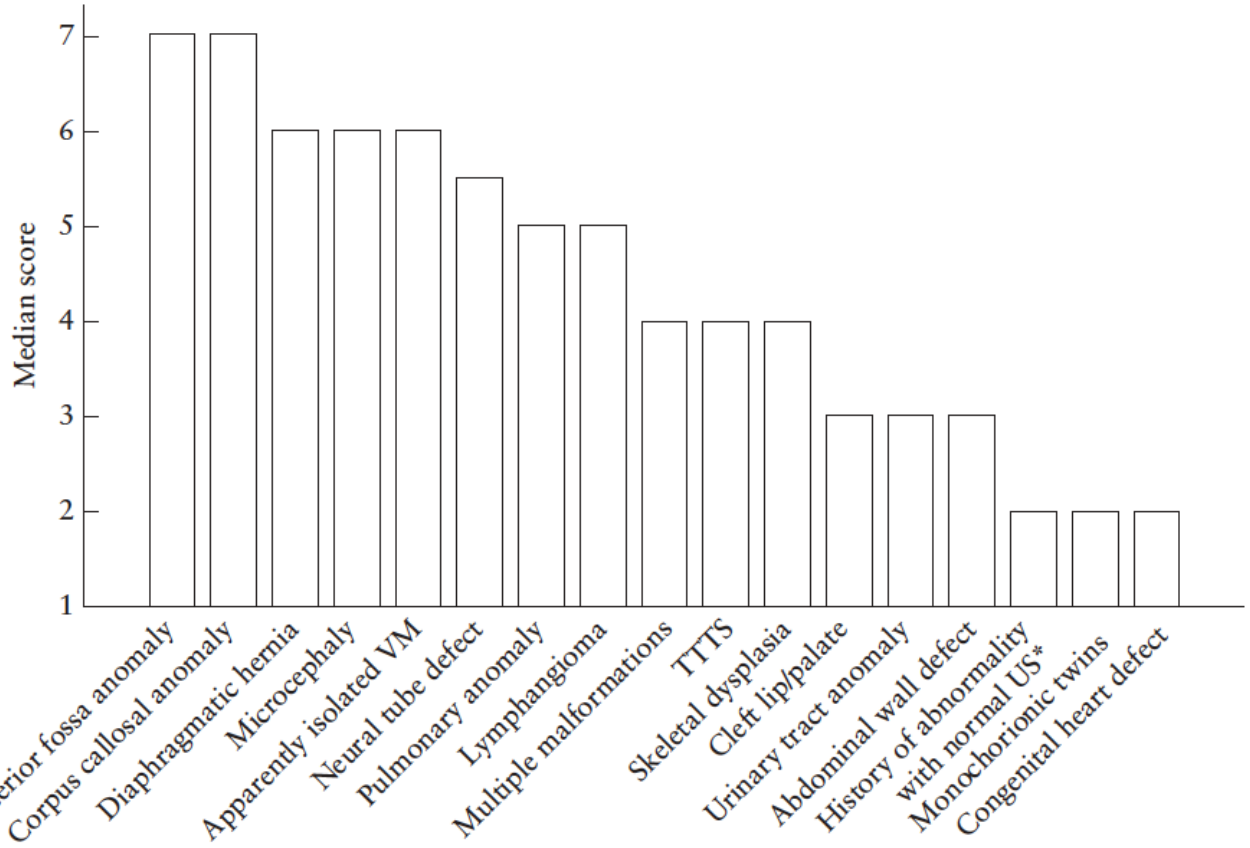

Figure 1 Results of ISUOG survey on indications for fetal magnetic resonance imaging (MRI), rated on a scale from 0 (fetal MRI not at all indicated) to 7 (definitely an indication for fetal MRI). *History of abnormality in previous pregnancy or in family member, with normal ultrasound (US) findings in current pregnancy. TTTS, twin–twin transfusion syndrome; VM, ventriculomegaly.

MRI FETAL

CERPO

<18 semanas: No provee información adicional a US.

20-22 semanas: Útil como complemento al US para evaluación y manejo en la sospecha de anomalías

3er trimestre: EG óptima para evaluación cortical cerebral y evaluación de VA en masas cervicales.

ISUOG Practice Guidelines: Performance of fetal magnetic resonance imaging. 2017

MRI - PASOS

Table 2 Steps in performance of fetal magnetic resonance imaging (MRI)

Indication	Dependent on quality of previous ultrasound examinations, clinical question and gestational age
Counseling of pregnant woman	Explanation of indication, performance, expected outcome and consequences of the procedure, information about the possibility of an accompanying person, discussion with respect to contraindications and claustrophobia and sedative drug prescription if necessary
Prerequisites for MRI unit	Written referral with clear indication of clinical question(s), ultrasound report and images (if possible), gestational age confirmed/determined by first-trimester ultrasound
At the MRI unit	Clarification of possible contraindications, comfortable positioning of woman (either supine or lateral decubitus position), adequate coil positioning, performance of examination according to pertinent protocol
After examination	Inform patient about when the report will be ready; in the case of immediate consequences resulting from MRI examination, information regarding results should be provided promptly to the referring physician
Storage of images, report	Electronic storage of images, analysis of images, structured reporting (Table 3)

ISUOG Practice Guidelines: Performance of fetal magnetic resonance imaging. 2017

PASOS: Previo a MRI

- Excluir contraindicaciones.
- Obtener consentimiento informado.
- Confirmar EG, evaluación clínica previa y hallazgos en US.
- Considerar sedantes para disminuir MF y/o artefactos. Uso también en pacientes ansiosas o claustrofóbicas.
- Posición cómoda para la paciente.
- Considerar acompañante.

ISUOG Practice Guidelines: Performance of fetal magnetic resonance imaging. 2017

PASOS: Durante MRI

- Adquirir secuencias.
- Asegurar localización correcta de la bobina en el órgano de interés en el centro de ésta.
- Evaluar el órgano de interés.
- Proceder a realizar evaluación fetal y extrafetal completa.
- Informar condiciones que requieran intervención inmediata.

ISUOG Practice Guidelines: Performance of fetal magnetic resonance imaging. 2017

MRI

Table 3 Structured report for detailed fetal magnetic resonance imaging examination

Method	Imaging conditions (e.g. degradation by fetal movement, maternal obesity, premature termination of examination), field strength, coil, sequences, planes
Head	Profile, hard and soft palate (Figure 6), skull, ocular measurements
Brain	Age-related sulcation and gyration, lamination of brain parenchyma (after 30 weeks: myelination and premyelination), ventricular system, cerebellum, midline structures and width of cerebrospinal fluid spaces (Figure 3)
Chest	Configuration of thorax, lung signals, gross regularity of heart (not examined in detail) (Figure 7a,b)
Abdomen	Fetal situs, stomach and gallbladder (fluid filling), fluid and meconium signals of bowels (Figure 7c,d), kidneys, urinary bladder (fluid filling); on request: female/male external genitals (in case of latter: descent of testes) (Figure 8)
Extrafetal structures	Umbilical cord (number of vessels), amount of amniotic fluid, position and characteristics of placenta, cervical length (Figure 9) only if substantially shortened
Skeleton (when examined)	Course and completeness of spine, shape, length and position of bones, fingers and toes (not always possible to assess, especially in presence of minimal amniotic fluid, i.e. after 32–35 weeks)

ISUOG Practice Guidelines: Performance of fetal magnetic resonance imaging. 2017

SEGURIDAD

- Sin efectos adversos a 1,5 T, en ningún momento del embarazo.
- Exposición en el 1er T no se asocia a mayor daño fetal vs no exposición.
- Uso de gadolinio se asocia con: Afección cutánea reumatológica, inflamatorias o infiltrativas y morbimortalidad neonatal.

Ray JG, Vermeulen MJ, Bharatha A, Montanera WJ, Park AL. Association between MRI exposure during pregnancy and fetal and childhood outcomes. JAMA 2016; 316: 952–961.

INDICACIONES

- Sistema nervioso central.
- Cráneo, cara y faringe.
- Masas cervicales y bocio fetal.
- Tórax.
- Abdominal.
- Tracto urogenital.
- Patología placentaria.

SNC

- Ventriculomegalia
- Defectos de la línea media
- Agenesia del cuerpo calloso
- Anomalías de la fosa posterior
- Malformaciones corticales cerebrales
- Esclerosis tuberosa
- Lisencefalia
- Anomalías médula espinal

Reddy UM, Abuhamad AZ. Fetal imaging: Executive summary of a Joint Eunice Kennedy Shriver National Institute of Child Health and Human Development, Society for Maternal-Fetal Medicine, American Institute of Ultrasound in Medicine, American College of Obstetricians and Gynecologists, American College of Radiology, Society for Pediatric Radiology, and Society of Radiologists in Ultrasound Fetal Imaging Workshop. Am J Obstet Gynecol 2014; 210: 387–397.

Table 1 Sensitivity, specificity, positive (PPV) and negative (NPV) predictive values of ultrasound, neurosonography and magnetic resonance imaging (MRI) in predicting postnatal outcome

Method	*Sensitivity (%)*	*Specificity (%)*	*PPV (%)*	*NPV (%)*
Referral ultrasound	55	20	55	20
Neurosonography	96	87	93	93
MRI	85	80	88	75

Table 5 Patients in whom magnetic resonance imaging proved more accurate than neurosonography

		Neurosonography		*MRI*		
Patient	*Referral ultrasound*	*Finding*	*Week*	*Finding*	*Week*	*Follow-up*
1	AV	AV	25	Ventriculomegaly, large SAS	28	TOP, ventriculomegaly
2	AV	AV	22	Normal ventricles	27	Delivered, normal imaging and development
3	AV	MV, third ventricular dilatation	23	MV	25	Delivered, normal imaging and development

AV, asymmetric ventriculomegaly; MRI, magnetic resonance imaging; MV, mild ventriculomegaly; SAS, subarachnoid space; TOP, termination of pregnancy.

Malinger G, Ben-Sira L, Lev D, Ben-Aroya Z, Kidron D, Lerman-Sagie T. Fetal brain imaging: a comparison between magnetic resonance imaging and dedicated neurosonography. Ultrasound Obstet Gynecol 2004; 23: 333–340.

Table 2 **More details of the surviving twins with brain abnormalities on *in utero* magnetic resonance in the treated twin–twin transfusion syndrome group**

Case	Summary	Ultrasound findings	iuMR findings	Outcome
T1	Laser ablation at 21 weeks; demise of one twin at 24 weeks	Referral USS at 24 weeks	iuMR at 25 weeks	Livebirth 35w
		Mild VM	Mild VM	
T3	Laser ablation at 18 weeks; demise of one twin before 19 weeks	Referral USS at 22 weeks	iuMR at 25 weeks	Livebirth 38w
		Normal	Generalised reduction of volume and of the left hemisphere and focal infarction in the frontal lobe; abnormal neural tissue lining the infarcted area consistent with reparative polymicrogyria (Figure 1)	
T6	Laser ablation at 24 weeks; demise of one twin before 25 weeks	Referral USS at 29 weeks	iuMR at 32 weeks	Born at 32w. Neonatal death
		Normal	Micrencephaly; extensive encephalomalacia, poor sulcation and abnormal cortex consistent with extensive reparative polymicrogyria	
T22	Laser ablation at 20 weeks; it is not known when the co-twin died, but both were alive at 27 weeks.	Referral USS at 31 weeks	iuMR at 32 weeks	Stillbirth at 32w
		Normal	Focal infarction in the left paracentral lobule with abnormal neural tissue in the adjacent tissue – probably reparative polymicrogyria (Figure 3)	

iuMR, *in utero* magnetic resonance; USS, ultrasound scan; VM, ventriculomegaly.

Griffiths PD, Sharrack S, Chan KL, Bamfo J, Williams F, Kilby MD. Fetal brain injury in survivors of twin pregnancies complicated by demise of one twin as assessed by in utero MR imaging. Prenat Diagn. 2015 Jun;35(6):583-91.

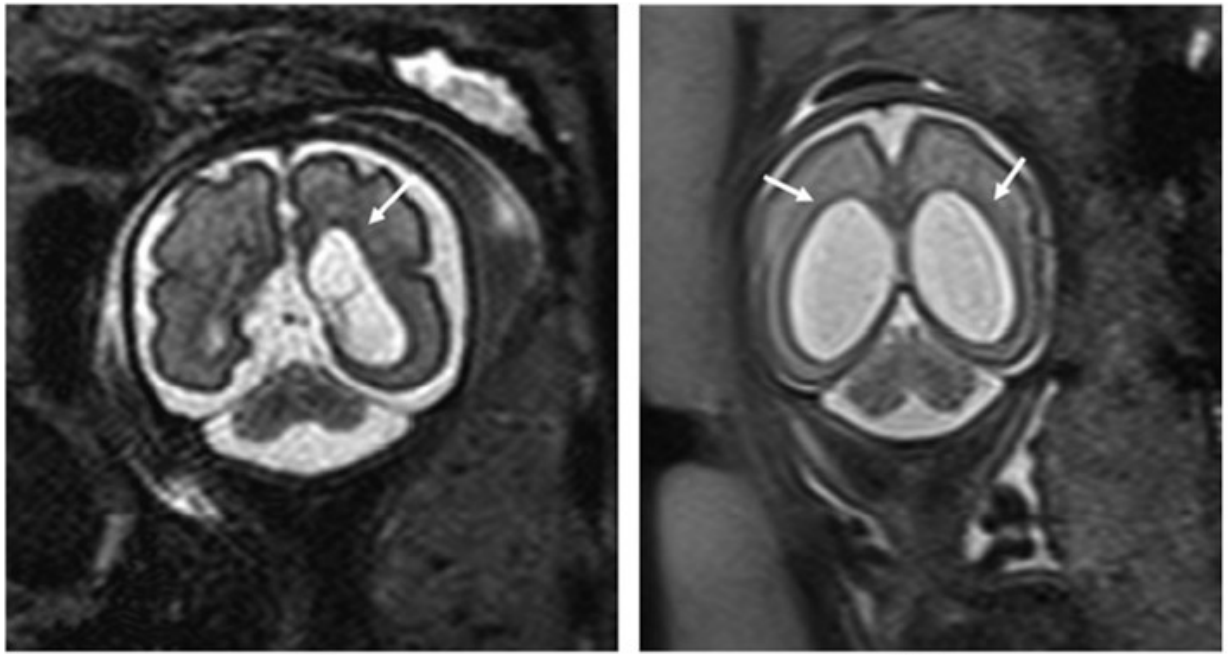

Figure 4 (a) SS-FSE T2W coronal image shows mild isolated left ventriculomegaly of 13 mm in a 29-week-old fetus. (b) Severe bilateral ventriculomegaly measuring 20 mm bilateral in a 29-week-old fetus with confirmed trisomy 21.

G. Masselli , Vaccaro Notte b, A. Zacharzewska-Gondek. Fetal MRI of CNS abnormalities. Clinical Radiology . 2020.

CERPO

C

F

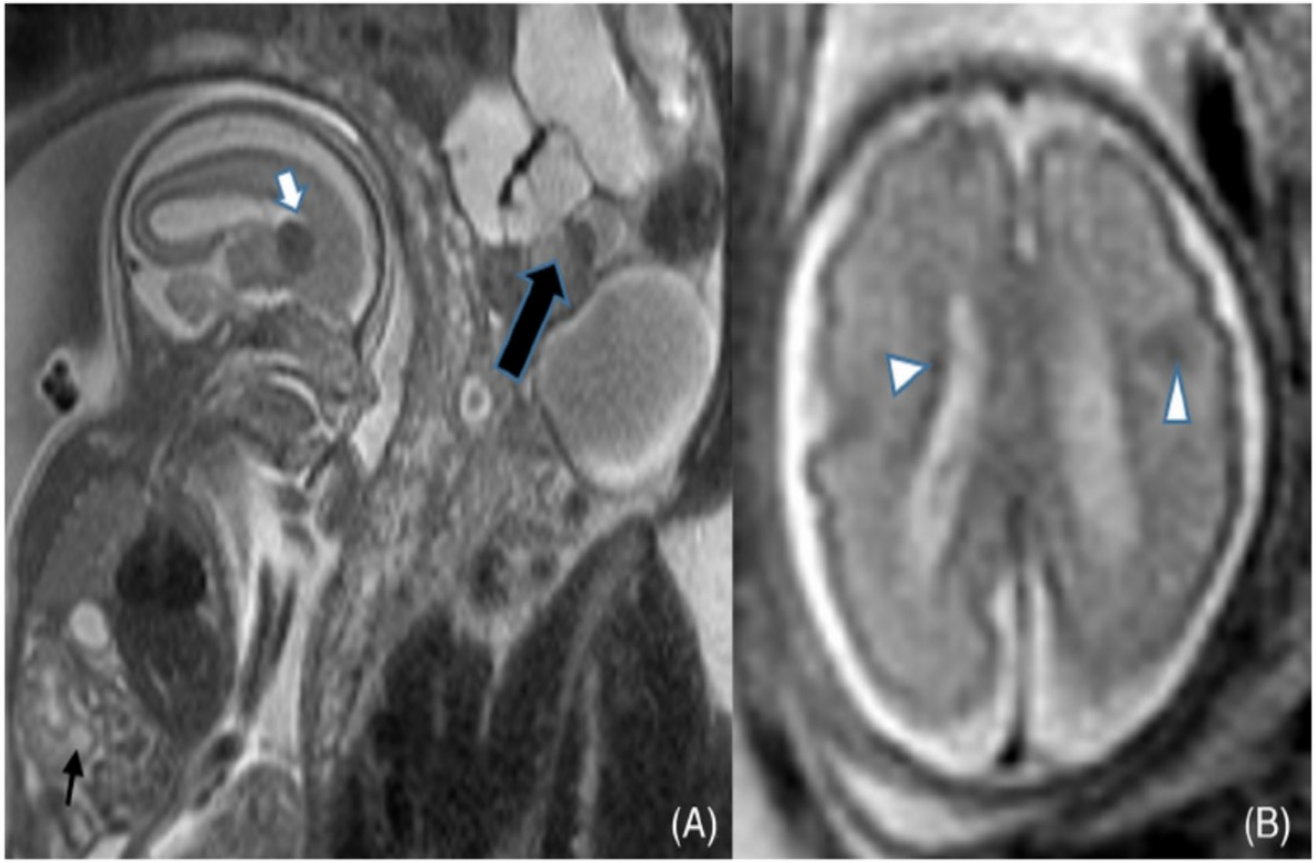

FIGURE 3 Fetal tuberous sclerosis complex (TSC). A, Sagittal and B, axial HASTE images show subependymal giant cell astrocytoma (SEGA) at the foramen Monro (white arrows), cortical tuber (long arrowhead), periventricular subependymal nodules (arrowhead) and renal angiomyolipomas (AML) (small black arrow). A mother is also diagnosed with TSC manifested with AML (large black arrow) [Colour figure can be viewed at wileyonlinelibrary.com]

Feygin T, Khalek N, Moldenhauer JS. Fetal brain, head, and neck tumors: Prenatal imaging and management. Prenat Diagn. 2020 Apr 30.

CRÁNEO, CARA Y OROFARINGE

Craneosinostosis	Cefalocele	Anomalía vasculares
Tumores	Microftalmia	Anomalias orbitarias
Fisura labiopalatina	Retrognatia	Micrognatia

Patenaude Y, Pugash D, Lim K, Morin L, Bly S, Butt K, Cargill Y, Davies G, Denis N, Hazlitt G, Naud K, Ouellet A, Salem S. The use of magnetic resonance imaging in the obstetric patient. J Obstet Gynaecol Can 2014; 36: 349–363.

Table 2—Comparison of ultrasound and MRI diagnoses

	Sonographic diagnosis	MRI diagnosis	Postnatal diagnosis
Case 1	Unilateral cleft lip–cleft alveolus	Unilateral cleft lip with anterior cleft palate	Unilateral cleft lip with anterior cleft palate
Case 2	Bilateral cleft lip–cleft alveolus	Bilateral cleft lip with anterior cleft palate	Bilateral cleft lip with anterior cleft palate
Case 3	Bilateral cleft lip–cleft alveolus	Bilateral cleft lip with full-length defect of the palate	Bilateral cleft lip with full-length defect of the palate
Case 4	Bilateral cleft lip–cleft alveolus	Bilateral cleft lip with full-length defect of the palate	Bilateral cleft lip with full-length defect of the palate
Case 5	Unilateral cleft lip–cleft alveolus	Unilateral cleft lip with anterior cleft palate; secondary palate not visualized	Unilateral cleft lip with anterior cleft palate
Case 6	Bilateral cleft lip–cleft alveolus	Bilateral cleft lip with anterior cleft palate; secondary palate not visualized	Bilateral cleft lip with full-length defect of the palate

Prenat Diagn 2003; **23**: 970–975.

Ghi T, Tani G, Savelli L, Colleoni GG, Pilu G, Bovicelli L. Prenatal imaging of facial clefts by magnetic resonance imaging with emphasis on the posterior palate. Prenat Diagn. 2003 Dec 15;23(12):970-5.

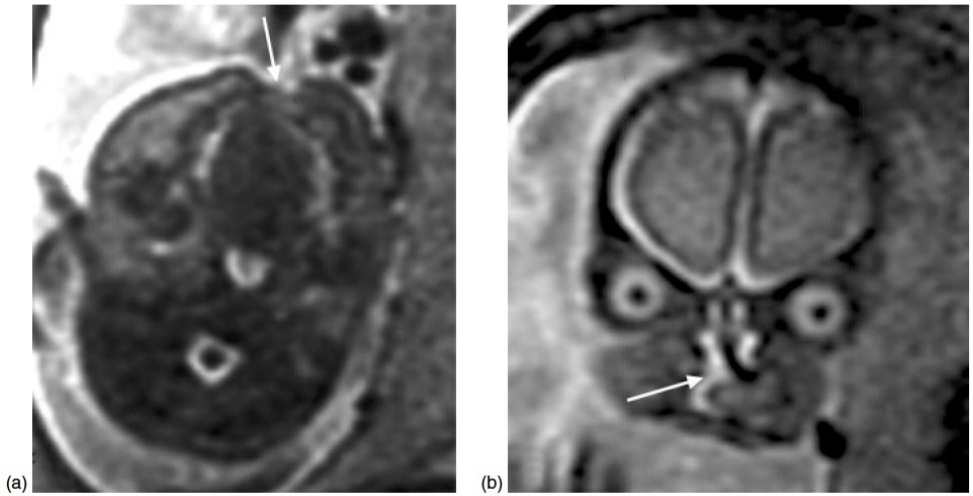

Figure 3—T2-weighted MRI of a fetus with unilateral cleft lip and palate: (a) the defect in the lip (arrow) is imaged in the axial section and (b) coronal view: the nose is distorted contralaterally to the cleft lip (arrow) and this indicates the involvement of the anterior palate (alveolus)

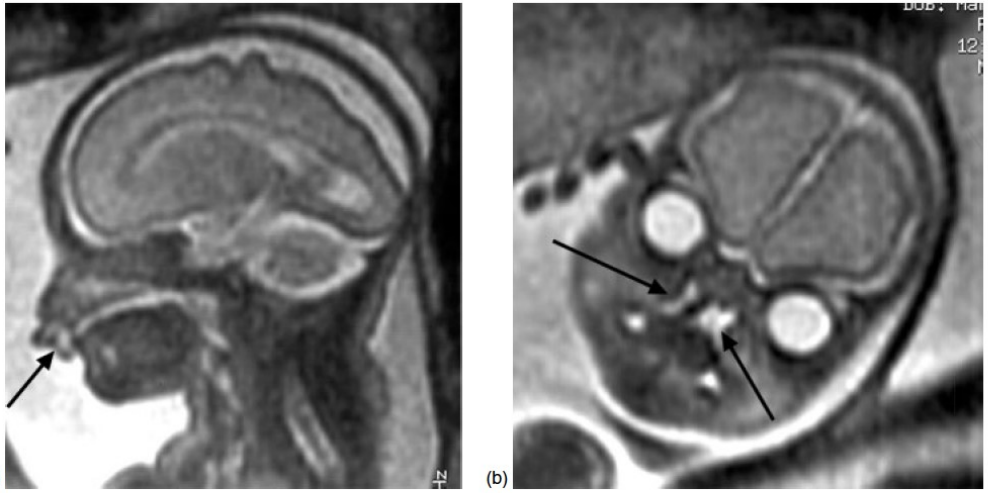

Figure 4—T2-weighted MRI of a fetus with bilateral cleft lip and palate: (a) protrusion of the premaxilla is clearly demonstrated in the sagittal view (arrow) and (b) a bilateral defect of the lip is documented in the coronal view (arrows); the distorted nose indicates the involvement of the anterior palate (alveolus)

Ghi T, Tani G, Savelli L, Colleoni GG, Pilu G, Bovicelli L. Prenatal imaging of facial clefts by magnetic resonance imaging with emphasis on the posterior palate. Prenat Diagn. 2003 Dec 15;23(12):970-5.

CUELLO

Masas cervicales

Bocio fetal

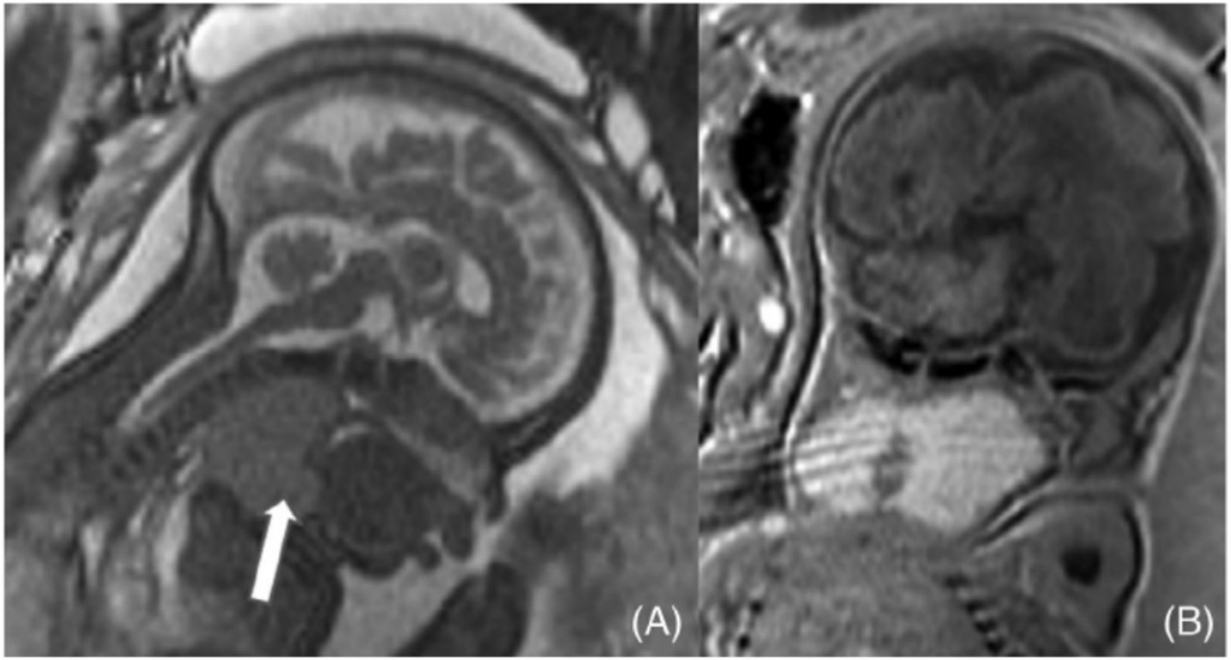

FIGURE 13 Fetal goiter. Fetal sagittal TRUE FISP (A) and coronal T1 (B) images show solid, bi-lobed, homogeneous, mid-line mass in the anterior neck (arrow) with typical high signal on T1-weighted images

Feygin T, Khalek N, Moldenhauer JS. Fetal brain, head, and neck tumors: Prenatal imaging and management. Prenat Diagn. 2020 Apr 30.

TÓRAX

Secuestro broncopulmonar

MAQ

Hernia diafragmática

Hipoplasia pulmonar

Patenaude Y, Pugash D, Lim K, Morin L, Bly S, Butt K, Cargill Y, Davies G, Denis N, Hazlitt G, Naud K, Ouellet A, Salem S. The use of magnetic resonance imaging in the obstetric patient. J Obstet Gynaecol Can 2014; 36: 349–363.

MRI: HDC

- Utilidad para HDC izquierda, discutible en HDC derecha.
- MRI mejor AUC que US.
- O/E VPF por MRI y LHR por US son útiles para predicción de sobrevida, desarrollo pulmonar y necesidad de ECMO.

Jani J, Cannie M, Sonigo P, Robert Y, Moreno O, Benachi A, Vaast P, Gratacos E, Nicolaides KH, Deprest J. Value of prenatal magnetic resonance imaging in the prediction of postnatal outcome in fetuses with diaphragmatic hernia. Ultrasound Obstet Gynecol. 2008 Nov;32(6):793-9.

HDC

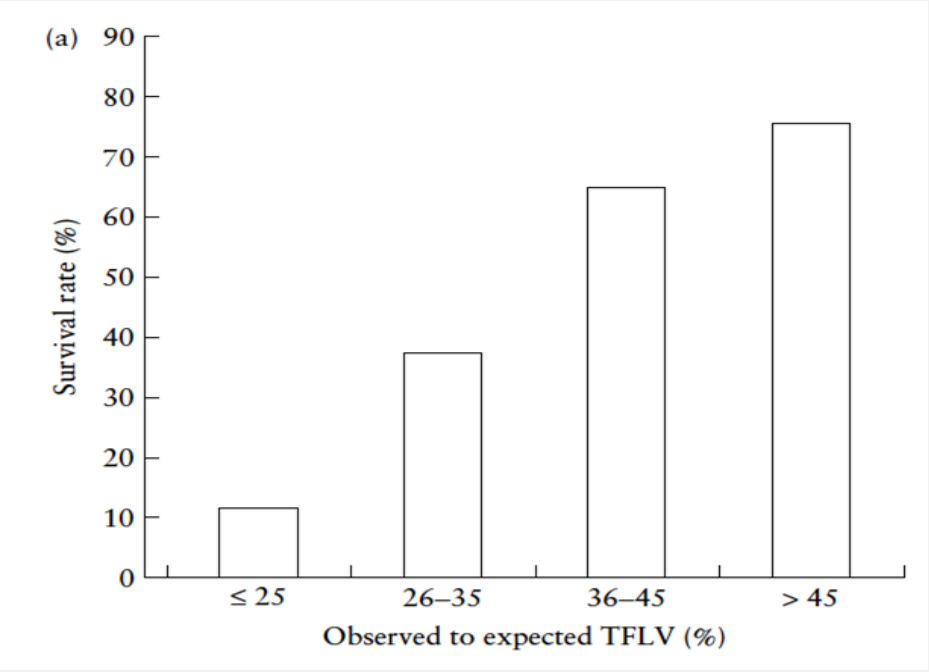

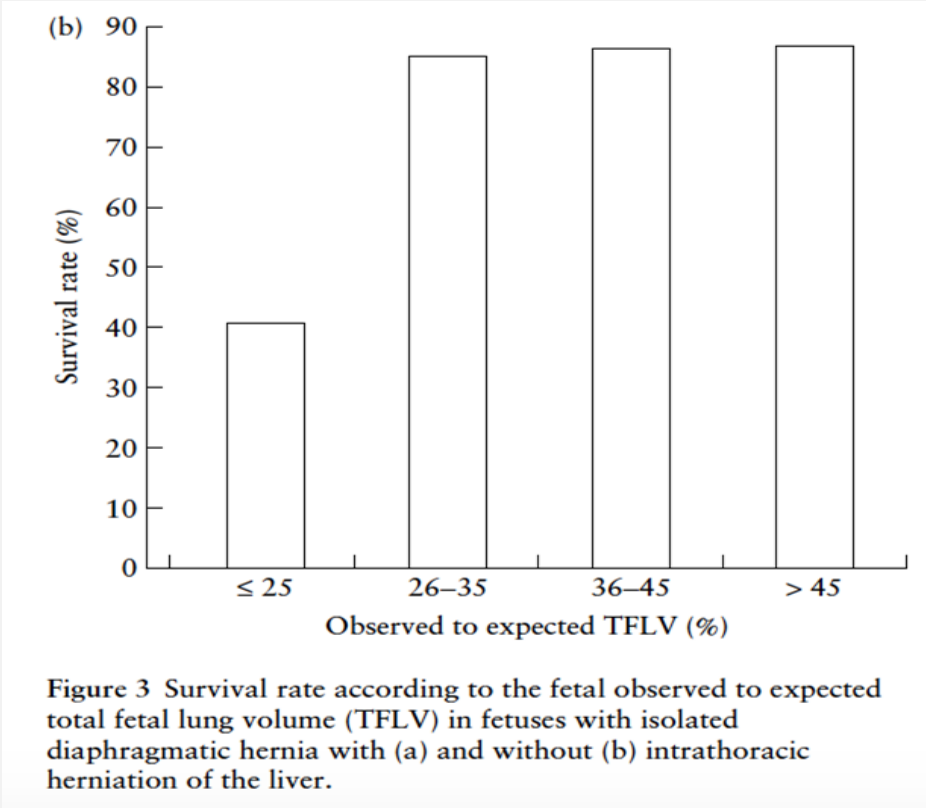

Figure 3 Survival rate according to the fetal observed to expected total fetal lung volume (TFLV) in fetuses with isolated diaphragmatic hernia with (a) and without (b) intrathoracic herniation of the liver.

Jani J, Cannie M, Sonigo P, Robert Y, Moreno O, Benachi A, Vaast P, Gratacos E, Nicolaides KH, Deprest J. Value of prenatal magnetic resonance imaging in the prediction of postnatal outcome in fetuses with diaphragmatic hernia. Ultrasound Obstet Gynecol. 2008 Nov;32(6):793-9.

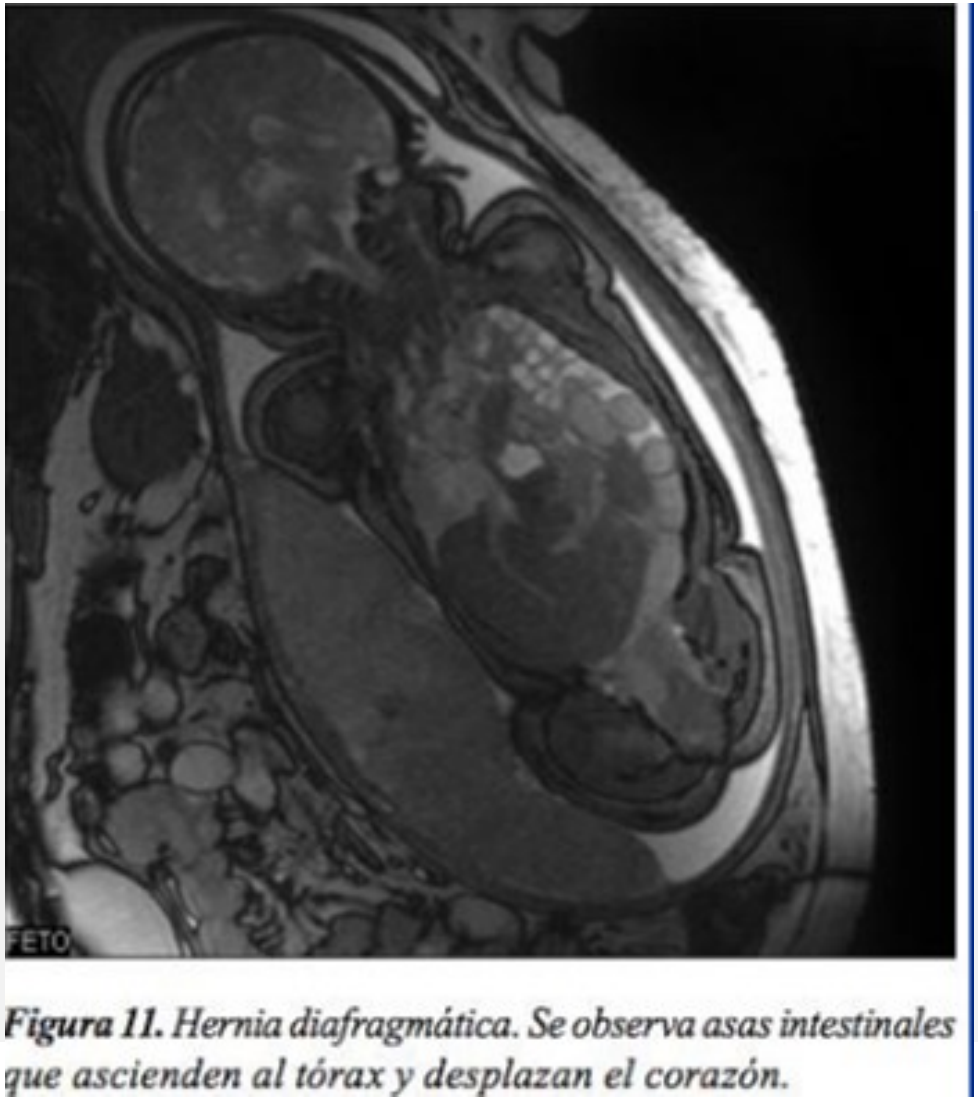

Figura 11. *Hernia diafragmática. Se observa asas intestinales que ascienden al tórax y desplazan el corazón.*

Muñoz, H., Parra, M., Ortega, X. Gomez, Ricardo. Resonancia magnética en obstetricia,

Fig. 1. A representative image of an axial single shot fast spin echo (SSFSE) T2-weighted MR image of a fetus with CLM. Using a freehand region of interest (ROI) tool the lung lesion and normal fetal lung areas were outlined. The lung lesion was identified as the region of most hyperintense signal in the chest.

Zamora IJ, Sheikh F, Cassady CI, Olutoye OO, Mehollin-Ray AR, Ruano R, Lee TC, Welty SE, Belfort MA, Ethun CG, Kim ME, Cass DL. Fetal MRI lung volumes are predictive of perinatal outcomes in fetuses with congenital lung masses. J Pediatr Surg 2014; 49: 853–858; discussion 858.

Table 2 Sensitivity and specificity of prenatal MRI in the diagnosis of congenital lung lesions according to various types of diagnoses. *BPS* Bronchopulmonary sequestration, *CPAM* congenital pulmonary airway malformation, *CI* confidence interval

	Sensitivity		Specificity	
Lesion type	(%)	95% CI	(%)	95% CI
CPAM	100	(87.5, 100)	96.6	(82.2, 99.9)
BPS[a]	66.7	(22.3, 95.7)	100	(92.9, 100)
BPS[b]	100.0	(54.1, 100)	96	(86.3, 99.5)
Hybrid	90.0	(55.5, 98.2)	100	(92.3, 100)
Overinflation[a]	81.8	(48.2, 97.7)	100	(92.1, 100)
Overinflation[c]	100.0	(71.5, 100)	95.6	(84.9, 99.5)
Bronchogenic cyst	100	(15.8, 100)	100	(93.4, 100)

[a] Indeterminate lesions were designated as "BPS or Overinflation" but had no prenatal diagnosis

[b] Indeterminate lesion was designated as "BPS or Overinflation" but had a prenatal diagnosis of BPS

[c] Indeterminate lesion was designated as "BPS or Overinflation" but had a prenatal diagnosis of overinflation

Pacharn P, Kline-Fath B, Calvo-Garcia M, Linam LE, Rubio EI, Salisbury S, et al. Congenital lung lesions: prenatal MRI and postnatal findings. Pediatr Radiol 2013;43:1136–43.

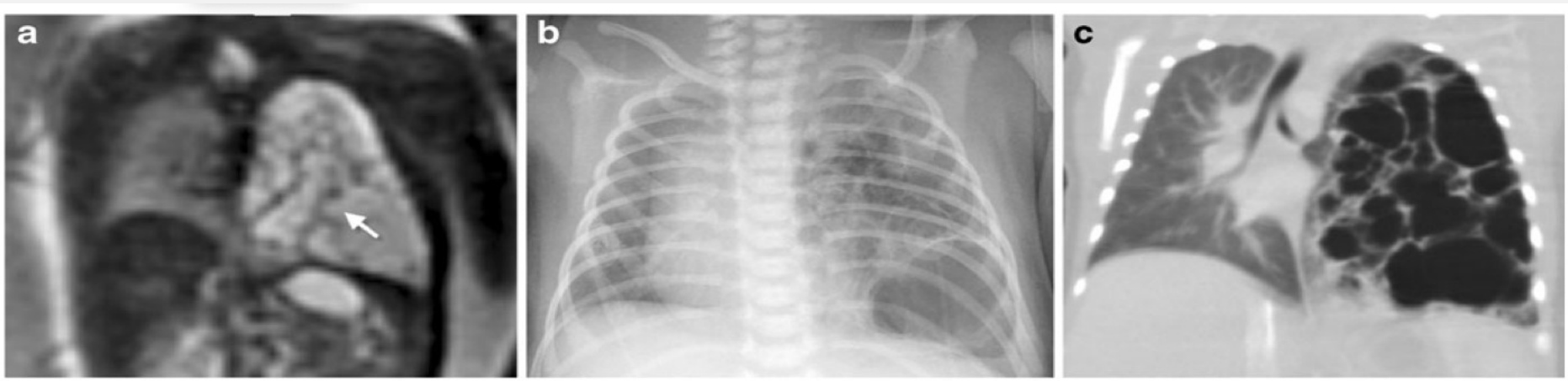

Fig. 2 CPAM. **a** Coronal single-shot fast spin-echo (SSFSE) MR image of a 24-week-old fetus. Fetal chest image demonstrates a large heterogeneous hyperintense mass in the left lung. The lesion contains multiple cysts and has pulmonary arterial vascular architectural distortion (*arrow*). Findings are consistent with CPAM type II. **b** Postnatal chest radiograph in the same patient demonstrates left lung mass containing multiple thin-walled air-filled cysts with associated right shift of the heart and mediastinum. **c** Postnatal coronal reformatted chest CT demonstrates multiple air-distended cysts of varying sizes in the left lower lobe consistent with CPAM. There is a shift of the tracheobronchial tree to the right

Zamora IJ, Sheikh F, Cassady CI, Olutoye OO, Mehollin-Ray AR, Ruano R, Lee TC, Welty SE, Belfort MA, Ethun CG, Kim ME, Cass DL. Fetal MRI lung volumes are predictive of perinatal outcomes in fetuses with congenital lung masses. J Pediatr Surg 2014; 49: 853–858; discussion 858.

ABDOMEN

Obstrucción intestinal

Malformaciones anorectales

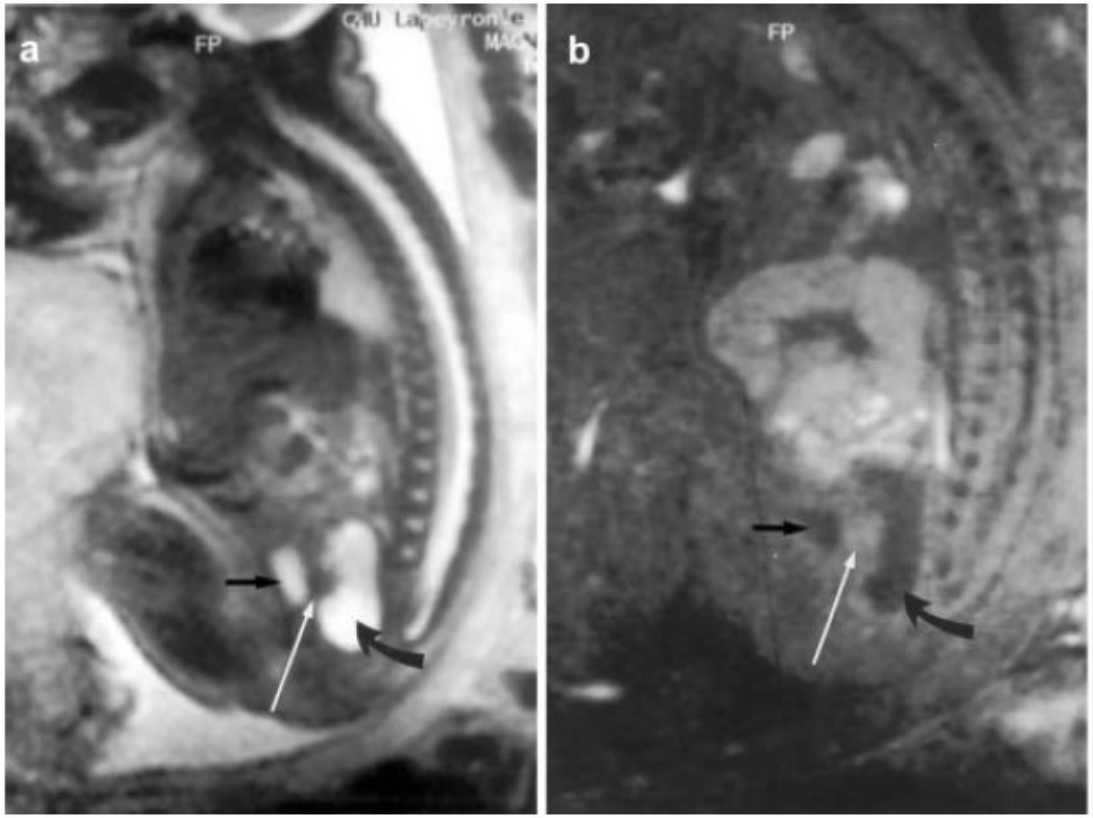

Fig. 11a–c. Cloacal malformation; 28 weeks' gestation. **a** Sagittal HASTE and **b** sagittal TI-W sequences demonstrate that the rectum (*curved arrow*) is moderately dilated and exhibits an abnormal liquid signal. It is normally located under the bladder neck, but is separated from the bladder (*short arrow*) by a structure with low signal on the T2-W sequence (**a**) and intermediate signal on the T1-W sequence (**b**), which corresponds to the dilated genital tract (*white arrow*). **c** Contrast medium introduced through a single orifice (*open white arrow*) at post-mortem fills the rectum (*curved arrow*), the urinary bladder (*short black arrow*) and dilated left genital tract (*white arrow*). Left ureteric reflux (*large white arrow*) is also present

Saguintaah M, Couture A, Veyrac C, Baud C, Quere MP. MRI of the fetal gastrointestinal tract. Pediatr Radiol. 2002 Jun;32(6):395-404.

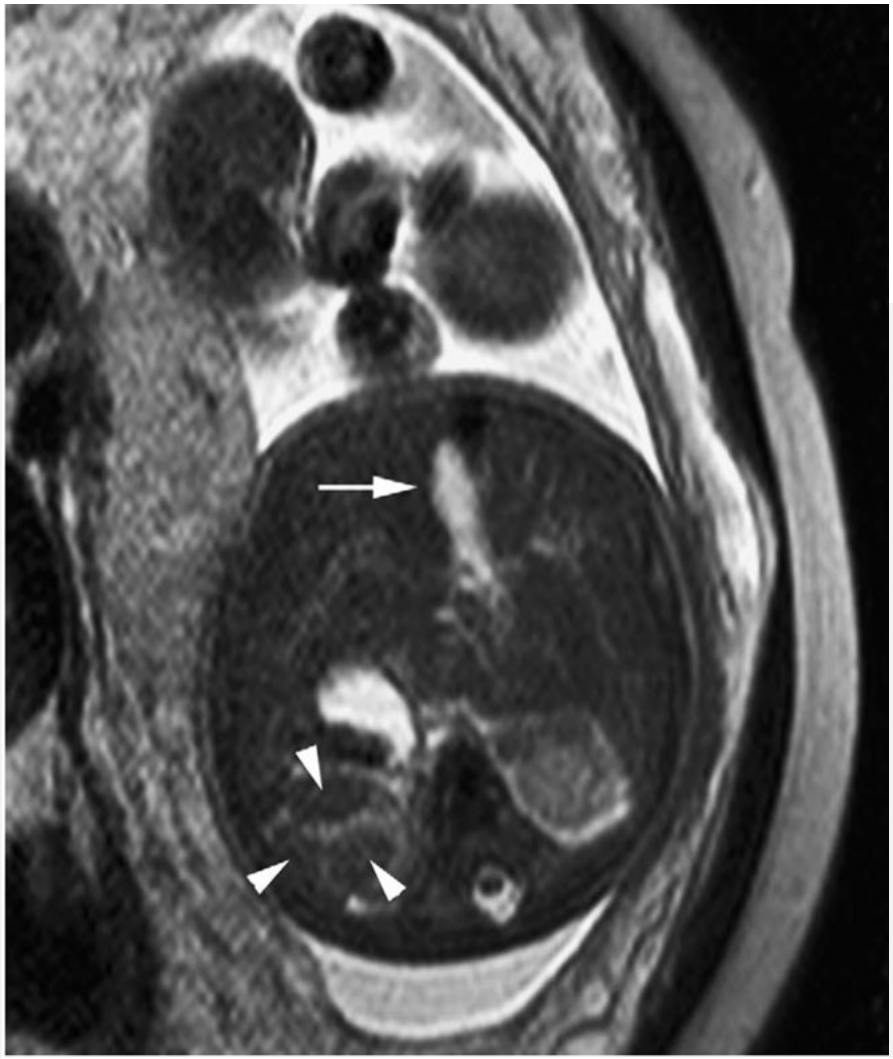

Fig. 17. Fetus at 28 GW with heterotaxy syndrome (left-sided isomerism) and abdominal situs inversus. Axial T2-weighted image demonstrates polysplenia with at least three spleens (arrowheads). Note also nearly median-positioned gallbladder (arrow).

Brugger PC, Prayer D. Fetal abdominal magnetic resonance imaging. Eur J Radiol 2006;57:278–93.

TRACTO UROGENITAL

Patología renal

Oligohidroamnios

Table 1
Correlation between the prenatal US and MRI findings and the final clinical diagnosis.

	US findings	MRI findings	Final diagnosis	Time of delivery and management
1. (26)	Left multicystic renal dysplasia	Left multicystic renal dysplasia	Left multicystic renal dysplasia	39 weeks, Rx, US, CUM, NM
2. (25)	Anamnios, renal and vesical agenesis and lungs hypoplasia	Anamnios. Renal and vesical agenesis. Lungs hypoplasia	Anamnios. Renal and vesical agenesis. Lungs hypoplasia	Abortion 26 weeks, autopsy
3. (20)	Anamnios, renal and vesical agenesis, lungs hypoplasia, and stomach agenesis	Anamnios. Renal and vesical agenesis. Lungs hypoplasia, stomac agenesis	Anamnios. Renal and vesical agenesis. Lungs hypoplasia. stomac agenesis	34 weeks, perinatal death, autopsy
4. (25)	Anamnios, renal and vesical agenesis	Anamnios. Renal and vesical agenesis. **Right lung agenesis**. **Severe left lung hypoplasia**	Anamnios. Renal and vesical agenesis. Right lung agenesis, Severe left lung hypoplasia	Abortion 26 weeks, autopsy
5. (32)	Oligoamnios, right renal agenesis versus dysplasia renal, and normal left kidney	Oligoamnios, **R kidney agenesis. normal left kidney**	R kidney agenesis. Normal left kidney	38 weeks, post-natal US and CUM
6. (23)	Oligoamnios, bilateral genu recurvatum, microcystis, right hydronephrosis, and left kidney normal	Oligoamnios, Bilateral genu recurvatum, microcystis, right hydronephrosis, **left kidney agenesis**, **tethered cord**	Bilateral genu recurvatum, Microcystis, right hydronephrosis, left kidney agenesia, tethered cord, polyslenia, clinodactylia	Abortion 23 weeks, autopsy
7. (29)	Left hydronephrosis and megaureter. Microcystis, right renal multicystic dysplasia	Left hydronephrosis and megaureter. Microcystis. Right renal multicystic dysplasia. **partial sacrum agenesis**	Left hydronephrosis and megaureter. Microcystis. Right renal multicystic dysplasia. Partial sacrum agenesis, ano-rectal malformation	39 weeks, Rx, US, CUM, MRI Colostomy
8. (29)	Left diaphragmatic hernia and horseshoe kidney	Left diaphragmatic hernia. **Ectopic left kidney. Left lung hypoplasy**	Left diaphragmatic hernia. Ectopic left kidney. Left lung hypoplasy	37 weeks, perinatal death, autopsy
9. (33)	Left diaphragmatic hernia and malrotated left kidney	Left diaphragmatic hernia, malrotated left kidney	Left diaphragmatic hernia, malrotated left kidney	35 weeks, Rx, US, CUM
10. (21)	Facial anomalies, double aortic arch, and hydronephrosis, horseshoe kidney	Facial anomalies, double aortic arch, hydronephrosis, renal malrotation	Facial anomalies, double aortich arch, hydronephrosis, horseshoe kidney	Abortion 21, 5 weeks, autopsy
11. (21)	Megacystis, post-urethral valves	Megacystis, Post-urethral valves. **Bilateral lung hypoplasia**. **Left cystic lung lesions**	Prune-Belly syndrome, megacystis, post-urethral valves. Bilateral lung hypoplasia. Left cystic lung lesions	Abortion 22 weeks, Autopsy
12. (26)	Post-urethral valves No identification of fetal sex Bilateral hydronehrosis and urinoma Suspicion of intestinal pathology	Post-urethral valves Micropenis Bilateral hydronephrosis and urinoma **Urachus persistence** **Bladder rupture** **No intestinal pathology** **Light lung hypoplasia**	Post-urethral valves Micropenis Bilateral hydronephrosis and urinoma Urachus persistence Bladder rupture No intestinal pathology	36 weeks Rx, US, CUM
13. (36)	Bilateral hydronephrosis. Pelvic cystic (ovarian) mass	Bilateral hydronephrosis **Mucocolpos** **Vaginal obstruction**	Bilateral hydronephrosis Mucocolpos Imperforate hymen.	37 weeks Rx, US Post-natal operation
14. (35)	Bilateral hydronephrosis Pelvic cystic (ovarian) mass	Bilateral hydronephrosis **Mucocolpos** **Vaginal obstruction**	Bilaterl hydronephrosis Mucocolpos Imperforate hymen.	35 weeks Rx, US Post-natal operation
15. (28)	Bilateral ovarian cysts	Bilateral ovarian cysts	Bilateral ovarian cysts	40 weeks, Rx, US

In the first column and between parentheses, the weeks of gestation at the time of prenatal MRI. In bold letters the additional information obtained by MRI. Modification of the US diagnosis after MRI occurred for cases 6, 8, 12, 13 and 14. Modification of the therapeutic approach after MRI was seen for cases 6, 11, 12, 13 and 14. Both imaging methods failed to recognize the ano-rectal malformation present in case 7. Bold words indicates the additional information obtained by MRI.

Alamo L, Laswad T, Schnyder P, Meuli R, Vial Y, Osterheld MC, Gudinchet F. Fetal MRI as complement to US in the diagnosis and characterization of anomalies of the genito-urinary tract. Eur J Radiol. 2010 Nov;76(2):258-64.

PLACENTA

- Acretismo placentario (posterior)

Table 2. Summary estimates of sensitivity, specificity, positive and negative likelihood ratios (LR^+ and LR^-) and diagnostic odds ratio (DOR) of magnetic resonance imaging (MRI) to detect each degree of placental invasion. Computations were based upon hierarchical summary receiver operating characteristic (HSROC), or DerSimonian–Laird random-effect model (Ψ).

	N. studies (sample)	References	Sensitivity % (95% CI)	Specificity % (95% CI)	DOR (95% CI)	LR^+ (95% CI)	LR^- (95% CI)
1. Placenta accreta	5 (175)	33,35,37–39	94.4 (15.8–99.9)	98.8 (70.7–100)	1397 (2.27–861,017)	79.4 (2.23–2835)	0.06 (0.00–4.00)
2. Placenta increta[Ψ]	3 (163)	33,35,38	100 (75.3–100)	97.3 (93.3–99.3)	297 (36.8–2402)	22.1 (9.64–50.6)	0.11 (0.03–0.50)
3. Placenta accreta+increta	8 (261)	28,31,33–35,37–39	95.0 (86.0–99.0)	96.0 (92.3–98.3)	95.3 (19.1–476)	28.3 (8.40–95.9)	0.0 (0.0–8.01)
4. Placenta percreta	7 (269)	28,29,31,33,34,37,38	86.5 (74.2–94.4)	96.8 (93.5–98.7)	80.3 (17.9–358)	16.5 (2.89–94.1)	0.25 (0.15–0.44)

CI, confidence interval.

Table 3. Measures of Test Accuracy in Patients Receiving Ultrasonography or Magnetic Resonance Imaging to Diagnose Placenta Accreta

	Sensitivity	Specificity	LR Positive	LR Negative	PPV	NPV
Magnetic Resonance Imaging	88.46 (86–100)	100 (76–100)	∞	0.115 (0.039–0.33)	100 (85–100)	82.35 (56–96)
Ultrasonography	76.92 (60–88)	96.13 (93–97)	19.9 (11.94–33.15)	0.24 (0.135–0.42)	65.21 (49–78)	97.78 (95–98)

LR, likelihood ratio; PPV, positive predictive value; NPV, negative predictive value.
Data are expressed as percentage (95% confidence interval).

Warshak CR, Eskander R, Hull AD, Scioscia AL, Mattrey RF, Benirschke K, Resnik R. Accuracy of ultrasonography and magnetic resonance imaging in the diagnosis of placenta accreta. Obstet Gynecol. 2006 Sep;108(3 Pt 1):573-81.

Familiari A, Liberati M, Lim P, Pagani G, Cali G, Buca D, Manzoli L, Flacco ME, Scambia G, D'antonio F. Diagnostic accuracy of magnetic resonance imaging in detecting the severity of abnormal invasive placenta: a systematic review and meta-analysis. Acta Obstet Gynecol Scand. 2018.

DISCUSIÓN

- Excelente complemento diagnóstico para US.
- Desventaja su disponibilidad y costo.
- Fundamental en la evaluación de las anomalías del SNC y torácica (HDC).
- Indicada, realizada e interpretada correctamente contribuye al diagnóstico, consejería, tratamiento y planificación del nacimiento.

CERPO

Centro de Referencia Perinatal Oriente

Facultad de Medicina, Universidad de Chile

Seminario N°87: Resonancia magnética fetal

Dr Heinz Dauelsberg Noemi,
Dr Daniel Martin Navarrete,
Mayo 2022